

1 ***In Silico* Identification of a Potent Arsenic Based Approved Drug Darinaparsin**
2 **against SARS-CoV-2: Inhibitor of RNA dependent RNA polymerase (RdRp)**
3 **and Necessary Proteases**

4 Trinath Chowdhury¹, Gourisankar Roymahapatra², Santi M. Mandal^{1,*}

5 ¹Central Research Facility, Indian Institute of Technology Kharagpur, Kharagpur 721302,
6 India.

7 ²School of Applied Science, Haldia Institute of Technology, Haldia 721657, India.

8

9

10

11 *Corresponding Author: Santi M. Mandal, Central Research Facility, Indian Institute of
12 Technology Kharagpur, Kharagpur 721302, India. Telephone: 91-3222 -282486, Fax: 91-
13 3222-282486. E. mail:mandalsm@gmail.com

14

15

16 **Short Title:** Darinaparsin against novel Corona virus

17

18

19

20

21

22

23 **Abstract**

24 COVID-19 is a life threatening novel corona viral infection to our civilization and
25 spreading rapidly. Terrific efforts are giving by the researchers to control the rate of
26 mortality. Here, a series of arsenical derivatives were optimized and analyzed with *in silico*
27 study to search the inhibitor of novel-corona viral replication or to stop the life cycle. All the
28 derivatives were blindly docked using iGEMDOCK v2.1 individually with RNA dependent
29 RNA polymerase (RdRp) of SARS-CoV-2, is the main component of viral replication and
30 appears to be the primary target of antiviral drugs. Based on the lower idock score in the
31 catalytic pocket of RdRp, darinaparsin (-82.52 kcal/mol) revealed most effective among
32 them. Darinaparsin strongly binds with both Nsp9 replicase protein (-8.77 kcal/mol) and
33 Nsp15 endoribonuclease (-8.3 kcal/mol) of SARS-CoV-2 as confirmed from the AutoDock
34 analysis. During infection, the ssRNA of SARS-CoV-2 is translated into large polyproteins
35 forming viral replication complex by specific proteases like 3CL protease and papain
36 protease. This is also another target to control the virus infection where darinaparsin also
37 perform the inhibitory role to proteases of 3CL protease (-7.69 kcal/mol) and papain protease
38 (-8.43 kcal/mol). In host cell, there is a protease named furin which serves as a gateway to the
39 viral entry and darinaparsin also docked with furin protease which also revealed a strong
40 binding affinity with furin protease. This screening of potential arsenic drugs would help in
41 providing the fast *in-vitro* to *in-vivo* analysis towards development of therapeutics for SARS-
42 Co-V2. Moreover, our result is satisfying the drug repurposing approach as the proposed
43 drug, darinaparsin is recommended chemotherapeutic agent of lung cancer.

44

45

46 **Keywords:** COVID-19, novel-corona virus, arsenical drug, Darinaparsin, RNA dependent
47 RNA polymerase, SARS CoV-2 surface spike glycoprotein

48

49

50

51 Introduction

52 COVID-19 makes its own way around the World, which is caused by severe acute respiratory
53 syndrome coronavirus 2 (SARS-CoV-2). In world scenario, this has already killed around
54 two hundred thousands people from its introduction in Wuhan, China, in December. Several
55 thousands are in risky situation. There is no FDA-approved effective drug to treat COVID-19
56 yet. Doctors and researchers are searching for option to treat the disease and stop to multiply.
57 In China alone, about 300 clinical trials have been done with standard antiviral drugs
58 including antiviral therapies such as interferons, stem cells, traditional Chinese medicines and
59 blood plasma from people who have already recovered from the virus (Yan et al., 2020).

60 Favilavir is the first approved drug against coronavirus by The National Medical
61 Products Administration of China, which has shown some level of efficacy with minimal
62 toxic effect. I-Mab Biopharma is also developed an antibody, TJM2 targeting the cytokine
63 granulocyte-macrophage colony-stimulating factor (GM-CSF) for cytokine tempest in
64 COVID-19 patients (Science News, 2019). Airway Therapeutics is developing rhSP-D, a
65 novel human recombinant protein named AT-100 for the treatment of coronavirus which is
66 under evaluation with the Respiratory Diseases Branch of the National Institutes of Health
67 (Clinical Trials, 2020). Lopinavir is analyzed by Dayer et al. (2017) following molecular
68 docking analysis and observed it might have some potency against Coronavirus Infection. Liu
69 et al., (2020) proposed hydroxychloroquine, a derivative of chloroquine, is efficient drug to
70 fight against SARS-CoV-2 infection. Several institutions are ongoing to develop the vaccines
71 against COVID-19. It is an urgent need to search for the novel inhibitor molecules to stop the
72 life cycle of SARS-CoV-2.

73 The techniques, molecular docking (*in silico*) has been object wise used in medicinal
74 chemistry for the identification of possible derivatives as inhibitor molecule for target
75 specific proteins. A series of study on molecular docking was published to search for the
76 inhibitor of SARS-CoV-2 receptors Nsp9 replicase, main protease, NSP15 endoribnuclease
77 (Smith and Smith, 2020) and chymotrypsin-like protease (Lee et al., 2014; Berry et al., 2015),
78 mRNA polymerases (Elfiky et al., 2017), and helicase (Zaher et al., 2020). Upon entry of
79 virus within the cell, the genomic RNA is directly moved on translation for the production of
80 two polyproteins pp1a and pp1ab. These two polyproteins are responsible for the synthesis of
81 several essential nonstructural proteins (nsPs) including two proteases such as Chymotrypsin-
82 like protease (3CLpro)-nsP5 and a papain like protease (Ppro) -nsP3 (Hilgenfeld, 2014; Zhou

83 [et al., 2020](#)). These two proteases are accountable to generate rest of the critical nsPs
84 including helicase, methyltransferase, and RNA dependent RNA polymerase (RdRp) which
85 forms replication transcription complex (RTC), crucial for viral replication ([Cui et al., 2019](#)).
86 Several viral pathogens utilize host proteases for their maturation. Activation of bacterial
87 toxins requires cleavage by proteases of the infected host. Therefore, few host proteases are
88 potential target for therapeutic approach for a variety of viral infectious diseases. Furin, a
89 human protease helps for infection development by the cleavage of spike glycoprotein of the
90 SARS-CoV-2 ([Li et al., 2020](#)), therefore furin is also another promising target for therapeutic
91 intervention against SARS-CoV-2.

92 In the present study, the aim was to identify a possible therapeutic candidate to stop
93 the replication of SARS-CoV-2. A virtual drug screening approach was used followed by
94 molecular docking in between the target site of RNA dependent RNA polymerase (RdRp),
95 3CL protease, papain protease and human protease furin with structurally optimized several
96 organo-arsenic molecules. Among them, one arsenic (As) derivative darinaparsin is reported
97 anticancer drug revealed significant of use to stop the replication of SARS-CoV-2. Despite of
98 the several adverse effects of As exposure to human beings, different organo-As compounds
99 or their derivatives have been used for medical purposes for more than 2000 years ([Del Razo](#)
100 [et al., 2001](#)). Arsenic is a non-essential trace elements have been reported as the inhibitor of
101 viral replication *in vitro* ([Kuroki et al., 2009](#)).

102

103 **Materials and Methods**

104 **Geometry optimization and theoretical calculations**

105 Geometry optimization of the arsenic derivatives was performed at the B3LYP basis set
106 following LANL2Dz level of theory ([Samanta et al., 2013](#)). The number of imaginary
107 frequency of all the molecules turned out to be zero, implying that they correspond to
108 minimum energy structures on the potential energy surface. All computations were performed
109 using the GAUSSIAN 09 program package. The optimized structures were generated through
110 the GAUSSVIEW 6 package ([Gaussian 09, 2016](#)), and the optimized structures were used for
111 docking study. The thermodynamic stability of any chemical system, irrespective of its size,
112 may be assessed quantitatively from its ionization potential (I), electron affinity (A),
113 electronegativity (χ), and electrophilicity (ω). The global electrophilicity index (ω) is
114 calculated from the explicit formula [$\omega = \chi^2 / 2\eta$] involving electronegativity [$\chi = \frac{I+A}{2}$] ([Parr](#)

115 et al., 1999; Roymahapatra et al., 2012). The thermodynamic stability of molecular system
116 may be meaningfully justified from the scrutiny of their chemical hardness (η) and
117 electrophilicity (ω) values.

118

119 **Virtual Screening**

120 Twelve different arsenical optimized compounds [3-4 DDSA (3-4-DDSA (3,4-diacetyloxy-5-
121 dimethylarsanylsulfanyloxolan-2-yl)methyl acetate), 3-amino-4-hydro-arsonic acid, Arsenic
122 acid, Arsenous acid, Dimethyl-arsenic acid, Dimethyl arsenous acid, Darinaparsin, Mono-
123 methyl-arsenic acid, Mono-methyl-arsenous acid, p-arsinilic acid, roxarsone, tri-methyl-
124 arsenate] were selected for docking analysis against RdRp of SARS-CoV-2 for preliminary
125 screening.

126

127 **Molecular docking**

128 Molecular docking calculations were performed with two different software iGEMDOCK
129 (<http://gemdock.life.nctu.edu.tw/dock/igemdock.php>) (Hsu et al., 2011) for blind docking and
130 AutoDockVina (<http://vina.scripps.edu/>) (Trott et al., 2010) for site-specific docking. The
131 ligand and proteins were prepared for the calculation of AutoDock Tools (ADT) 1.5.6
132 (Morris et al., 2009). Water if present was removed first then hydrogens were added to both
133 receptor and ligand individually. Kollmann charges (receptor) and Gasteiger charges (ligand)
134 were then calculated by ADT followed by merging non-polar hydrogens. The grid box was
135 sized as 40 x 40 x 40 units based on the grid points in x, y and z axis. The grid boxes were
136 centered on the coordinates of residue atoms located in the region of active site and interface
137 region shown in Table 3. The grid maps were generated accordingly. The number of modes
138 was set to 50 and exhaustiveness was set to 24. While calculating docking parameters,
139 Arsenic (As) and Sodium (Na) were missing in the AD4_parameter.dat file. So a command
140 line was included for respective metals by calculating Rii (sum of vdW radii of two like
141 atoms (Å), epsii (vdW well depth in kcal/mol), vol (atomic solvation volume (Å³), solpar
142 (atomic solvation parameter), Rij_hb (H-bond radius of the heteroatom in contact with a
143 hydrogen), epsij_hb (well depth of H-bond in kcal/mol), hbond (integer indicating type of H-
144 bonding atom), rec_index (initialized to -1, but later on holds count of how many of this atom
145 type are in), map_index (initialized to -1, but later on holds the index of the AutoGrid map),
146 bond_index (used in AutoDock to detect bonds) before each dock run. The docking is based
147 on the criterion of efficiency of interaction, the complexes with binding energy values better

148 or equals to -7 kcal/mol. After successful docking the docked files were analyzed in PyMOL
149 software for visualization (Lill and Danielson, 2011).

150

151 **Results and Discussion**

152 Research institutions and pharmaceutical companies are developing vaccines against SARS-
153 CoV-2 (Hofmarcher et al., 2020). Incredible efforts are also given by a group of researchers
154 for the virtual screening and sometimes supercomputer-aided drug repositioning to search for
155 a novel inhibitor molecule to control the infection (Park et al., 2020). We have explored with
156 a new series of arsenic compounds to search for the inhibitor of corona virus replication. It
157 was reported that two metal oxides such as arsenic and antimony exhibited an excellent
158 antiviral properties on bacteriophage as confirmed with plaques formation assay in different
159 medium (Charan et al., 2012). The antiviral mechanism of As_2O_3 with potent activities
160 against the several viral strains has been well documented and proposed therapeutics to
161 cure from HCV infection (Hwang et al., 2004). This study highlights the indications for use
162 of an arsenical drug as anti-SARS-CoV-2 agent using a method of virtual screening and
163 molecular docking analysis.

164 From the primary screening to final obtained arsenical drug, darinaparsin is all respect
165 chose the most efficient antiviral drugs to inhibit corona virus infection by *in silico* study.
166 While optimizing all arsenical compounds, the conceptual density functional theory based
167 reactivity descriptors are widely used to determine the stability and reactivity of different
168 molecules. According to the Koopmans' theorem (Gu and Xu, 2020), the ionization potential
169 (I) and electron affinity (A) of a molecular system can be expressed in terms of the energies
170 of the frontier molecular orbital's (FMOs) as $I \approx -E_{HOMO}$ and $A \approx -E_{LUMO}$. In another way,
171 higher the band gap ($E_{HOMO} - E_{LUMO}$) higher the stability and lower the band gap more
172 reactive species is to be considered (Roymahapatra et al., 2012). These electronic structure
173 principles act as major determinants towards assessing the stability and reactivity trends of
174 different chemical system.

175 It is found that compounds, darinaparsin, 3-amino-4-hydroxy-arsonic acid, *p*-arsenilic
176 acid and roxarsone are the less stable more reactive among them and the reactivity order is *p*-
177 arsenilic acid>roxarsone>3-amino-4-hydroxy-arsonic acid >3-4-DDSA>darinaparsin (Table
178 1), although the data are calculated optimizing the compounds in gas phase and individual
179 molecular reactivity was considered, the trend may slightly varied in solvent phase or within

180 biological environment. This is exactly happened in our docking study. Compounds with ‘S’
181 atom (Table 2) are effective as antibacterial and antifungal. Our study shows that darinaparsin
182 show more effective among all tested molecules. Darinaparsin shows a very strong binding
183 affinity with bacterial cell due to strong electrostatic interaction. Darinaparsin (keto form)
184 having two (-CO-NH-) linkage can tautomerize to enol form (-C(OH)=N-) in reaction
185 intermediate. The keto form [$E_{0(\text{keto})} / E_{0(\text{enol})} = -1102.269 \text{ au} / -1102.195 \text{ au}$] is energetically
186 favorable in its ground state configuration having a good electronic mobility due to
187 tautomerization, which make darinaparsin towards strong binding agent with RdRp of
188 corona virus with strong electrostatic interaction.

189 The structural analysis of RdRp revealed that nsp(non structural protein) 12 complex
190 bound with nsp7 and nsp8 cofactors (Kirchdoerfer et al., 2019). The Nsp12 possess a
191 polymerase domain (amino acid position 398-919). The active site of RdRp domain
192 comprises A to G motifs, out of which Motif-A comprising residues of 611 to 626 as
193 TPHLMGWDYPKCDRAM. The classic divalent-cation binding residue D618 is conserved
194 in most of the viral polymerases (Appleby et al., 2015; Gong et al., 2010). Motif C residues
195 753-FSMMILSDDAVVCFN-767) contains the catalytic residues (759-SDD-761) in turn
196 between two β -strands (Gao et al., 2020). While screening of the arsenical compounds with
197 RdRp (PDB ID:6NUS) using blind docking method in iGEMDOCK software, darinaparsin
198 binds to the most appropriate catalytic domain in the region D618 of Motif A (a.a. 611-626)
199 of RdRp (Table 2).

200 After primary screening, six individual receptor proteins were targeted in this study as
201 i) Nsp9 replicase protein, ii) Nsp15 endoribonuclease protein, iii) 3CL protease, iv) papain-
202 like protease, v) furin protease. The SARS-CoV-2 replicase gene represented to encode
203 multiple enzymatic functions (Snijder et al., 2003). Nsp9 is present in the intracellular matrix
204 and helps in nuclear transport machinery. Its interaction with other proteins may be essential
205 for the formation of viral replication complex together with its ability to interact with RNA
206 (Sutton et al., 2004). *In silico* docking of darinaparsin with nsp9 replicase protein of SARS-
207 CoV-2 (PDB ID 6W4B) revealed a strong and significant binding affinity (Figure 2A). The
208 binding free energy was calculated as -8.77 kcal/mol (Table 3). Darinaparsin binds with the
209 interacting residues THR80, LYS82, LYS85 of nsp9 replicase protein (Figure 2B) resulting
210 in blocking the active site of the protein.

211 The virus encodes several unusual RNA processing enzymes, including Nsp15
212 endoribonuclease that preferentially cleaves 3' of uridylates through a ribonuclease A

213 (RNase)-like mechanism (Ortiz-Alcantara et al., 2010). Nsp15 endonuclease is a non-
214 structural protein 15 which is considered as an integral component of the coronaviral
215 replicase-transcriptase complex (RTC) with independent of endonuclease activity. The
216 catalytic site of Nsp15 is HIS250 where site-specific docking was performed. Docking of
217 darinaparsin with Nsp15 endoribonuclease (PDB ID:6VWW) showed a good binding affinity
218 of -8.3 kcal/mol (Table 3). The docking result confirms the following residues HIS250, LEU
219 246, GLY248, LEU249, GLY247, GLY239, LYS290 involved in the site of interaction
220 (Figure 2C and 2D).

221 Another attractive drug target of coronavirus is the main proteases due to its essential
222 role in processing the polyproteins that are translated from the viral RNA. Most of the
223 coronaviridae genome encodes two large polyproteins, pp1a and pp1ab, these polyproteins
224 are cleaved and transformed in mature non-structural proteins (Nsp) by the two proteases
225 3CLpro (3CLike protease) and PLpro (Papain Like Protease) encoded by the open reading
226 frame 1. NSPs, in turn, play a fundamental role in the transcription/replication during the
227 infection. Targeting these proteases is a valid approach for antiviral drug design. The
228 catalytically active site of 3CLpro is a dimer. Cleavage by 3CLpro occurs at the glutamine
229 residue in the P1 position of the substrate via the protease CYS-HIS dyad in which the
230 cysteine thiol functions as the nucleophile in the proteolytic process.

231 Figure 3A and 3B represents the docking of darinaparsin with 3CL protease (PDB ID:
232 6M2N). The amino residues GLY143, CYS145, GLU166 are the active site of binding of
233 3CL protease with a binding energy of -7.39 kcal/mol (Table 3). Apart from the active site
234 residues, darinaparsin also binds with ASN142, SER144, HIS163, LEU141. *In silico* docking
235 of papain-like protease (PDB ID: 3E9S) with darinaparsin form a complex with a binding
236 free energy -8.43 kcal/mol (Table 3). The interacting amino acid residues are ASP165,
237 PRO249, TYR265, GLY267, ASN268, TYR269, GLN270, TYR274 as revealed from
238 docking studies (Figure 3C and 3D). Similar type of docking was done with the main
239 protease of SARS-CoV-2 (PDB ID: 6Y84) with darinaparsin molecule. The complex
240 obtained a binding free energy of -7.19 kcal/mol (Table 3) by interacting with the residues
241 ASN142, GLY143, CYS145 (Figure 4A and 4B).

242 Human furin, a kind of proprotein convertases, can mediate S1/S2 cleavage unlike
243 other coronaviruses and contribute to membrane fusion efficiency which explains current
244 strong infectious capacity of SARS-CoV-2 (Walls et al.,2020; Canrong et al., 2020). *In silico*

245 docking study of furin protease (PDB ID: 4RYD) with darinaparsin also shows very good
246 result in terms of binding affinity. The binding free energy was calculated as -7.23 kcal/mol
247 (Table 3) having its catalytic site HIS300. Darinaparsin binds with the furin protease in the
248 residues GLY297, HIS300, ASP301, SER302, SER330 (Figure 4C and 4D). In light of this
249 finding, darinaparsin needs to be checked *in vitro* for clinical use as a successful drug
250 candidate to control the replication of SARS-CoV-2. Darinaparsin is an approved clinically
251 used anti-cancerous drug.

252 **Conclusion**

253 From the above docking and DFT study, it was revealed that darinaparsin molecule have a
254 strong and maximum binding affinity to RdRp of SARS-CoV-2 among the tested arsenical
255 compounds. This study also confirmed the significant interaction between the active site of
256 viral replicase protein, endoribonuclease protein and different proteases with darinaparsin.
257 Darinaparsin is also able to interact with human protease, furin which is another crucial
258 protease for viral entry. Thus darinaparsin an active compound among arsenical drugs may be
259 used as antiviral agent for COVID-19.

260

261 **References**

262 Appleby, T.C., Perry, J.K., Murakami, E., Barauskas, O., Feng, J., Cho, A., Fox D.3rd.,
263 Wetmore, D.R., McGrath, M.E., Ray, A.S., Sofia, M.J., Swaminathan, S., Edwards,
264 T.E. (2015). Structural basis for RNA replication by the hepatitis C virus polymerase.
265 *Science* 347:771–775. doi:10.1126/science.1259210 Medline

266 Berry, M., Fielding, B.C., Gamielien, J. (2015) Potential Broad Spectrum Inhibitors of the
267 Coronavirus 3CLpro: A Virtual Screening and Structure-Based Drug Design Study.
268 *Viruses*. 7(12):6642-60.

269 Canrong, W., Yang, L., Yueying, Y., Peng, Z., Wu, Z., Yali, W., Qiqi, W., Yang Y.,
270 Mingxue, M. et al., (2020) Analysis of therapeutic targets for SARS CoV-2 and
271 discovery of potential drugs by computational methods. *Acta Pharmaceutica Sinica B*.
272 <https://doi.org/10.1016/j.apsb.2020.02.008>

273 Centers for Disease Control and Prevention (a.n.d.) *Common Human*, (2019)
274 *oronaviruses*. <https://www.cdc.gov/coronavirus/general-information.html>

- 275 Charan, N., Lavanya, N., Praveen, B., Praveen, A., Sridevi, A., Golla, N. (2012). Antiviral
276 activity of antimony and arsenic oxides. *Der Pharma Chemica*. 4(2):687-689.
- 277 Clinical trials, Arnea (2020). [https://www.clinicaltrialsarena.com/analysis/coronavirus-mers-](https://www.clinicaltrialsarena.com/analysis/coronavirus-mers-cov-drugs/)
278 [cov-drugs/](https://www.clinicaltrialsarena.com/analysis/coronavirus-mers-cov-drugs/)
- 279 Corradia V., Mancinib M, Santuccib M.A., Carlomagnoc T., Sanfelicec D., Moria M.,
280 Vignarolia G., Falchia F., Manettia F., Radia M., Botta M. (2011) Computational
281 techniques are valuable tools for the discovery of protein–protein interaction inhibitors:
282 The 14-3-3 σ case *Bioorganic Medicinal Chemistry Letters*. 21(22):6867-71. doi:
283 10.1016/j.bmcl.2011.09.011.
- 284 Cui, J., Li, F., Shi, Z.L. (2019). Origin and evolution of pathogenic coronaviruses. *Nature*
285 *reviews Microbiology*, 17(3), pp.181-192.
- 286 Dayer, M.R., Taleb-Gassabi, S., Saaid Dayer, M. (2017). Lopinavir; A Potent Drug against
287 Coronavirus Infection: Insight from Molecular Docking Study. *Arch Clin Infect Dis*.
288 12(4):e13823.
- 289 Del Razo, L., Quintanilla-Vega, M. B., Brambila-Colombres, E., Calderon-Aranda, E.S.,
290 Manno, M., Albores, A. (2001). Stress proteins induced by arsenic. *Toxicol Appl*
291 *Pharmacol* 177:132-48.
- 292 Elfiky, A.A., Mahdy, S.M., Elshemey, W.M. (2017) Quantitative structure-activity
293 relationship and molecular docking revealed a potency of anti-hepatitis C virus drugs
294 against human corona viruses. *Journal of Medical Virology*. 89(6):1040-47.
- 295 Gao, Y., Yan, L., Huang, Y., Liu, F., Zhao, Y., Cao, L., Wang, T., Sun, Q., et al (2020)
296 Structure of RNA-dependent RNA polymerase from COVID-19 virus. *Science*. DOI:
297 10.1126/science.abb7498
- 298 Gaussian 09, Revision D.01, Gaussian, Inc., Wallingford CT, 2013. (b) Gaussian 16,
299 Revision C.01, Gaussian, Inc., Wallingford CT, 2016.
- 300 Gong, P., Peersen, O.B. (2010). Structural basis for active site closure by the poliovirus
301 RNA-dependent RNA polymerase. *Proc. Natl. Acad. Sci. U.S.A.* 107:22505–22510.
302 doi:10.1073/pnas.1007626107 Medline

- 303 Gu, Y., Xu, X. (2020). Extended Koopmaan's theorem at the second order perturbation
304 theory. *Journal of Computational Chemistry*. 41(12):1165-1174.
- 305 Hilgenfeld, R. (2014) From SARS to MERS: crystallographic studies on coronaviral
306 proteases enable antiviral drug design. *The FEBS Journal*, 281(18), pp.4085-4096.
- 307 Hofmarcher, M., Mayr, A., Rumetshofer, E., Ruch, P., Renz, P., Schimunek, J., Seidl, P.,
308 Vall, A., Widrich, M., Hochreiter, S., Klambauer, G. (2020). Large-scale ligand based
309 virtual screening for SARS CoV-2 inhibitors using deep neural networks.
310 *Biomolecules*. arXiv:2004.00979.
- 311 Hsu, K-C., Chen, Y-F., Lin, S-R., Yang, J-M. (2011). iGEMDOCK: a graphical environment
312 of enhancing GEMDOCK using pharmacological interactions and post screening
313 analysis. *BMC Bioinformatics*. 12, Article No.S33.
- 314 Hwang, D-R., Tsai, Y-C., Lee, J-C., Huang, K-K., Lin, R-K., Ho, C-H., Chiou, J-M., Lin, Y-
315 T., Hsu, J.T.A., Yeh, C-T. (2004). Inhibition of Hepatitis C virus Replication by Arsenic
316 Trioxide. *Antimicrobial Agents and Chemotherapy*.48(8):2876-2882.
- 317 Kirchdoefer, R.N., Ward, A.B. (2019). Structure of the SARS CoV nsp12 polymerase bound
318 to nsp7 and nsp8 co-factors. *Nature Communication*. 10(1):2342. doi: 10.1038/s41467-
319 019-10280-3.
- 320 Kuroki, M., Ariumi, Y., Ikeda, M., Dansako, H., Wakita, T., Kato, N. (2009). Arsenic
321 trioxide inhibits hepatitis C virus RNA replication through modulation of the
322 glutathione redox system and oxidative stress. *J Virol*. 83:2338-48.
- 323 Lee, H., Mittal, A., Patel, K., Gatuz, J.L., Truong, L., Torres, J et al. (2014). Identification of
324 novel drug scaffolds for inhibition of SARS-CoV 3-Chymotrypsin-like protease using
325 virtual and high-throughput screenings. *Bioorganic & Medicinal Chemistry*. 22(1):167-
326 77.
- 327 Li, W. (2020) A Furin Cleavage Site Inserted into the Spike Protein of SARS-CoV-2: A
328 Structural Implication?. *Preprints 2020*, 2020030428 (doi:
329 10.20944/preprints202003.0428.v1.

- 330 Lill, M.A., Danielson, M.L. (2011) Computer aided drug design platform using PyMOL.
331 Journal of Computer aided Molecular Design.25(1):13-19.
- 332 Liu, J., Cao, R., Xu, M., Wang, X., Zhang, H., Hu, H., Li, Y., Hu, Z., Zhong, W., Wang, M.
333 (2020) Hydroxychloroquine, a less toxic derivative of chloroquine, is effective in
334 inhibiting SARS-CoV-2 infection in vitro. Cell Discovery. 6:16.
- 335 Morris, G.M., Huey, R., Lindstrom, W., Michel, F.S., Richard, K.B., David, S.G., Arthur,
336 J.O. (2009). AutoDock4 and AutoDockTools4: Automated Docking with Selective
337 Receptor Flexibility. Journal of Computational Chemistry. 30:2785–2791.
338 <https://doi.org/10.1002/jcc.21256>
- 339 Ortiz-Alcantara, J., Bhardwaj, K., Palaninathan, S., Frieman, M., Baric, R.S., Kao, C.C.
340 (2010). Small molecule inhibitors of the SARS CoV Nsp15 endoribonuclease. Virus
341 Adaptation and Treatment. 2(1) <https://doi.org/10.2147/VAAT.S12733>
- 342 Parr, R.G., Szentpaly, Lv., Liu, S. (1999) Electrophilicity index. J. Am. Chem. Soc. 121:1922-
343 1924.
- 344 Roymahapatra, G., Mandal, S.M., Porto, W.F., Samanta, T., Giri, S., Dinda, J., Franco, O.L.,
345 Chattaraj, P.K. (2012). Pyrazine functionalized Ag(I) and Au(I)-NHC complexes are
346 potential antibacterial agents. Current Med. Chem., 19: 2012, 4184-4193
- 347 Samanta, T., Roymahapatra, G., Porto, W.F., Seth, S., Ghorai, S., Saha, S., Sengupta,
348 J., Franco, O.L., Dinda, J., Mandal, S.M. (2013). N, N'-Olefin functionalized bis-
349 imidazolium gold(I) salt is an efficient candidate to control keratitis-associated eye
350 infection. PLoS One. 2013;8(3):e58346.
- 351 Seo, Sangjao., Park, J.W., An, D., Yoon, J., Paik, H., Hwang, S. (2020) Supercomputer aided
352 Drug Repositioning at Scale: Virtual Screening for SARS-CoV-2 Protease Inhibitor.
353 Preprint.
- 354 Science News (2019) [https://www.sciencenews.org/article/coronavirus-covid19-repurposed-](https://www.sciencenews.org/article/coronavirus-covid19-repurposed-treatments-drugs)
355 [treatments-drugs](https://www.sciencenews.org/article/coronavirus-covid19-repurposed-treatments-drugs)
- 356 Smith, M., Smith, J.C. Repurposing Therapeutics for COVID-19: Supercomputer-Based
357 Docking to the SARS-CoV-2 Viral Spike Protein and Viral Spike Protein-Human
358 ACE2 Interface. ChemRxiv. 2020; Preprint.
359 <https://doi.org/10.26434/chemrxiv.11871402.v3>].

360 Snijder, E.J., Bredenbeek, P.J., Dobbe, J.C., Thiel, V., Ziebuhr, J., Poon, L.L., Guan, Y.,
361 Rozanov, M., Spaan, W.J., Gorbalenya, A.E. (2003). Unique and conserved features of
362 genome and proteome of SARS coronavirus, an early split-off from the coronavirus
363 group 2 lineage. *331(5):991-1004*.

364 Sutton, G., Fry, E., Carter, L.G., Sainsbury, S., Walter, T.S., Nettleship, J.E., Berrow, N.S.,
365 Owens, R.J., Gilbert, R. et al. (2004). The nsp9 Replicase protein of SARS coronavirus,
366 Structure and Functional Insights. *Structure, 12(2):3410353*.

367
368 Trott, O., Olson, A.J. (2010) AutoDock Vina: improving the speed and accuracy of docking
369 with a new scoring function, efficient optimization, and multithreading. *Journal of*
370 *Computational Chemistry.31:455–461*. <https://doi.org/10.1002/jcc.21334>

371 Walls, A.C., Park, Y-J., Tortorici, M.A., Wall, A., McGuire, A.T., Vessler, D. (2020)
372 Structure, Function and Antigenicity of the SARS CoV-2 Spike Glycoprotein. *Cell*.
373 *180:281-292*.

374 Yan, R., Zhang, Y., Li, Y., Xia, L., Guo, Y., Zhou Q. (2020) Structural basis for the
375 recognition of SARS-CoV-2 by full length human ACE2. *Science. 367(6485):1444-*
376 *1448*.

377 Zaher, N.H., Mostafa, M.I., Altaher, A.Y. (2020) Design, synthesis and molecular docking of
378 novel triazole derivatives as potential CoV helicase inhibitors. *Acta Pharmaceutica*.
379 *70(2):145-59*.

380 Zhou, Y., Hou, Y., Shen, J., Huang, Y., Martin, W. and Cheng, F. (2020). Network-
381 based drug repurposing for novel coronavirus 2019-nCoV/SARS-CoV-2. *Cell*
382 *Discovery. 6(1), pp.1-18*.

383
384

385 **Author contribution:** SMM conceived the idea and wrote the manuscript; TC performs
386 docking analysis; GM optimized the molecules and performs DFT analysis.

387 **Conflict of Interest:** Authors declare none conflict of interest.

388 **Financial statement:** No financial involved performing this work.

389

390 **Figure Legends:**

391

392 **Figure 1.** Docked image of RdRp (6NUS) of SARS coronavirus with Darinaparsin (A)
393 Zoomed image of ligand binding site involving the participation of catalytic pocket (ASP618)
394 in Motif A of RdRp. The yellow marked portion represent interaction site (B).

395 **Figure 2.** Docked image of Nsp9 RNA binding protein of SARS-CoV-2 (6W4B) with
396 Darinaparsin. The yellow marked portion represents interaction site (A) Amino residue
397 present in receptor-ligand binding site of interaction (B) Docked image of Nsp15
398 endoribonuclease of SARS CoV-2 (6VWW) with Darinaparsin. The yellow marked portion
399 represents interaction site (C) and Amino residue present in receptor-ligand interaction site
400 between Nsp15 and darinaparsin (D).

401 **Figure 3.** Docked image of SARS CoV-2 3CL-protease with Darinaparsin. The yellow
402 marked portion represents interaction site (A) Amino residues present in protein-ligand
403 interaction site between 3CL-protease with darinaparsin (B) Docked image of papain like
404 protease of SARS coronavirus (3E9S) with Darinaparsin. The yellow marked portion
405 represents interaction site (C) Amino residues present in receptor-ligand interaction site
406 between papain like protease with darinaparsin (D)

407

408 **Figure 4.** Docked image of SARS-CoV-2 main proteases (6Y84) with Darinaparsin. The
409 yellow marked portion represents interaction site (A) Amino residues involved in receptor-
410 ligand binding site between main protease with darinaparsin (B) Docked image of Furin
411 protease (4RYD) with Darinaparsin. The yellow marked portion represents interaction site
412 (C) Amino residue involved in receptor-ligand binding site of interaction (D).

413

414

415

416

417

418

419

420 Table 1. Computational and DFT analysis of the optimized studied compounds along with
 421 their stability and reactivity parameters.

Compd.	Energy (ev)	(HOMO-LUMO) (ev)	IP (I) (ev)	EA (A) (ev)	Electronegativity (χ) (ev)	Electrophilicity (ω) (ev)
arsenic acid	-308.778	0.2293	0.3112	0.0819	0.1966	0.0044
arsenous acid	-233.619	0.2686	0.2942	0.0257	0.1599	0.0034
mono-methyl-arsenic acid	-348.074	0.2281	0.3027	0.0746	0.1886	0.0041
di-methyl-arsenic acid	-387.371	0.2285	.2962	0.0678	0.1820	0.0038
mono-methyl-arsenous acid	-272.914	0.2594	0.2824	0.0230	0.1527	0.0030
di-methyl-arsenous acid	-312.205	0.2572	0.2707	0.0135	0.1421	0.0026
tri-methyl-arsenate	-426.666	0.2279	0.2897	0.0618	0.1757	0.0035
tri-methyl-arsineoxide	-201.041	0.2690	0.2324	-0.0366	0.0979	0.0013
Darinaprasin	-1102.269	0.1961	0.2366	0.0405	0.1386	0.0019
3-amino-4hydro-arsonic acid	-595.147	0.1747	0.2137	0.0390	0.1263	0.0014
<i>p</i> -arsenilic acid	-519.830	0.1173	0.1808	0.0635	0.1221	0.0009
Roxarsone	-744.247	0.1655	0.2869	0.1214	0.2042	0.0034
3-4-DDSA	-972.054	0.1854	0.2531	0.0678	0.1604	0.0024

422

423

424

425

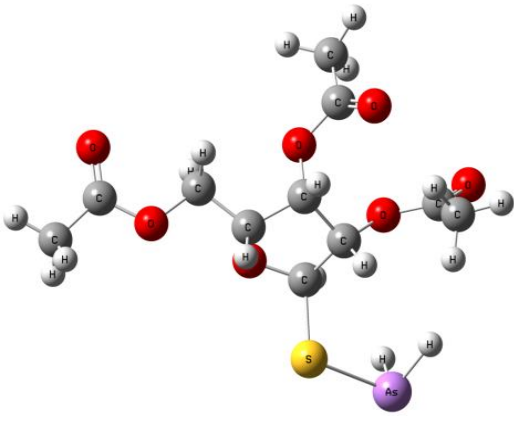
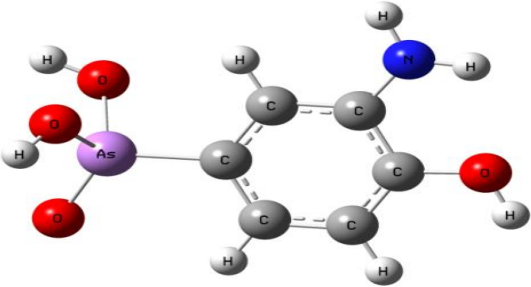
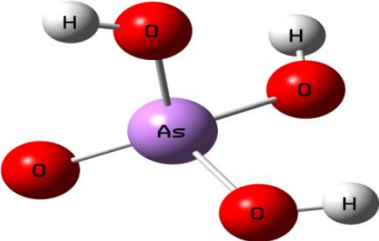
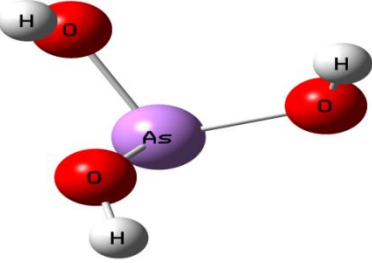
426

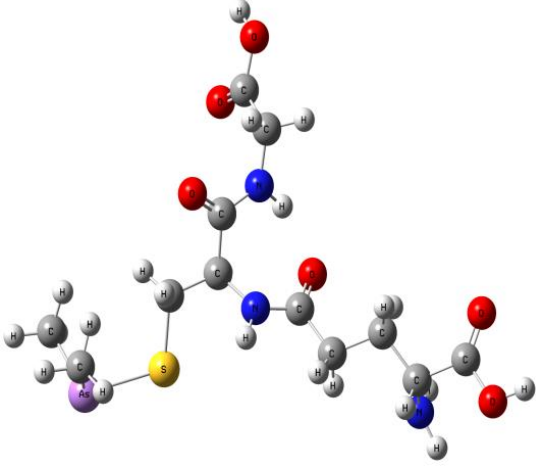
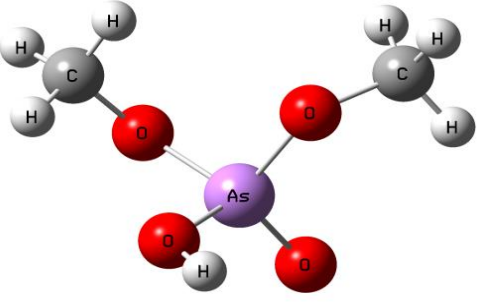
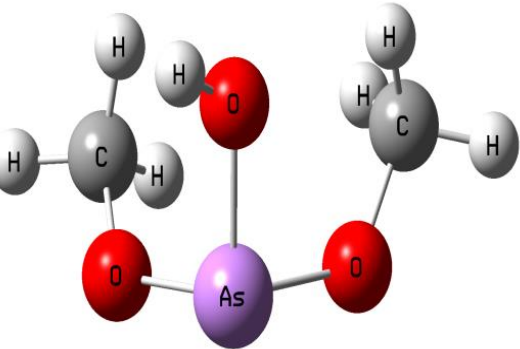
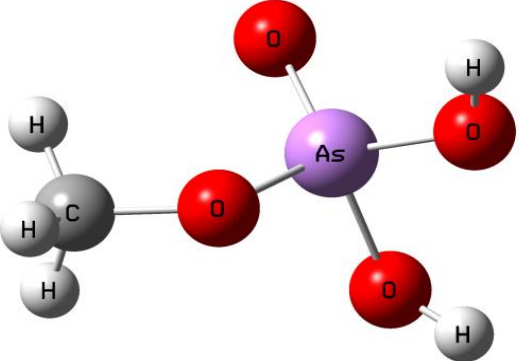
427

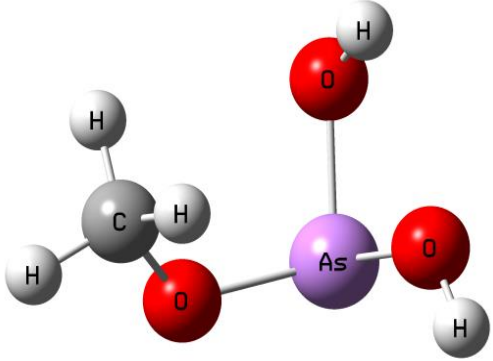
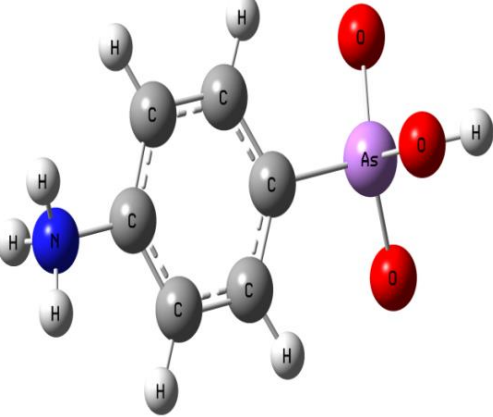
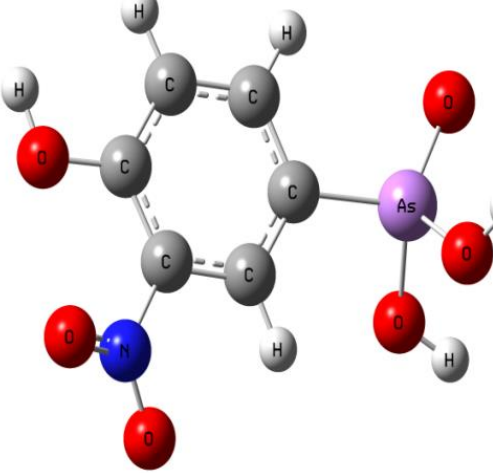
428

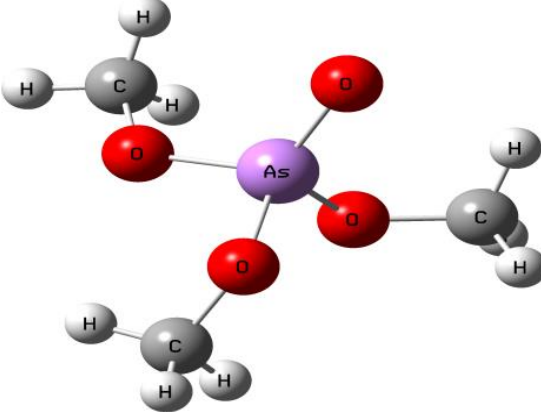
429

430 Table 2: Screening of different optimized arsenical compounds with SARS Coronavirus RdRp (6NUS)
 431 by blind docking using iGEMDOCK

Receptor	Ligand	Ligand Structure	Binding Free energy (kcal/mol)	Site of Interaction
6NUS- A chain (SARS Coronavirus Nsp12 polymerase)	3-4-DDSA		-68.58	SER592, MET601, ARG583, THR591, GLY597, ASN600.
6NUS- A chain (SARS Coronavirus Nsp12 polymerase)	3-amino-4hydro- arsonic acid		-71.43	HIS133, SER709, ASN781, LYS780.
6NUS- A chain (SARS Coronavirus Nsp12 polymerase)	Arsenic acid		-56.09	ARG631, SER681, ASP684, THR686, THR687.
6NUS- A chain (SARS Coronavirus Nsp12 polymerase)	Arsenous acid		-41.01	TRP617, ASN695.

6NUS- A chain (SARS Coronavirus Nsp12 polymerase)	Darinapa rsin		-82.52	TRP617, ASP618, ARG750, SER754, MET755, THR604.
6NUS- A chain (SARS Coronavirus Nsp12 polymerase)	Di-meth- arsenic acid		-45.24	ARG132, ASP465, GLN468, TYR732.
6NUS- A chain (SARS Coronavirus Nsp12 polymerase)	Di-meth- arsenous acid		-40.51	HIS133, SER709, ASN781.
6NUS- A chain (SARS Coronavirus Nsp12 polymerase)	Mono- meth- arsenic acid		-51.22	HIS133, SER709, ASN781.

6NUS- A chain (SARS Coronavirus Nsp12 polymerase)	Mono-meth-arsenous acid		-39.08	SER501, THR540, GLN541, VAL560.
6NUS- A chain (SARS Coronavirus Nsp12 polymerase)	p-arsenilic acid		-61.54	TYR129, HIS133, SER709, THR710, ASN781, ALA706, LYS780.
6NUS- A chain (SARS Coronavirus Nsp12 polymerase)	Roxarso ne		-70.58	GLY584, GLY597, ASN600, THR604, ARG583, MET601.

6NUS- A chain (SARS Coronavirus Nsp12 polymerase)	Tri-meth-arsenate		-50.1	HIS133, SER709, ASN781, LYS780.
---	-------------------	--	-------	---------------------------------

432

433

434

435

436

437

438

439

440

441

442

443

444

445

446

447

448

449

450

451

452 Table 3: Site specific interaction of darinaparsin with Nsp9 RNA binding protein, Nsp15
 453 endoribonuclease, main protease and 3CL-protease of SARS-Cov-2

454

Receptor	Ligand	Active Site / Catalytic site	Binding Free energy (kcal/mol)	Site of Interaction
6W4B:A – Nsp9 RNA binding protein of SARS-CoV-2	Darinaparsin	LYS85	-8.77	THR 80, LYS82, LYS85.
6VWW:A – Nsp15 Endoribonuclease of SARS-CoV-2	Darinaparsin	HIS250	-8.3	HIS250, LEU 246, GLY248, LEU249, GLY247, GLY239, LYS290.
6M2N:A – SARS-CoV-2 3CL-protease	Darinaparsin	GLY143, CYS145, GLU166	-7.69	ASN142, GLY143, SER144, CYS145, HIS163, LEU141, GLU166.
3E9S:A – Papain like protease	Darinaparsin	GLY267, ASN268, TYR269, GLN270	-8.43	ASP165, PRO249, TYR265, GLY267, ASN268, TYR269, GLN270, TYR274.
6Y84:A – SARS-CoV-2 Main Protease with unliganded active site	Darinaparsin	ASN142	-7.19	ASN142, GLY143, CYS145.
4RYD:A – Furin Protease	Darinaparsin	HIS300	-7.23	GLY297, HIS300, ASP301, SER302, SER330.

455

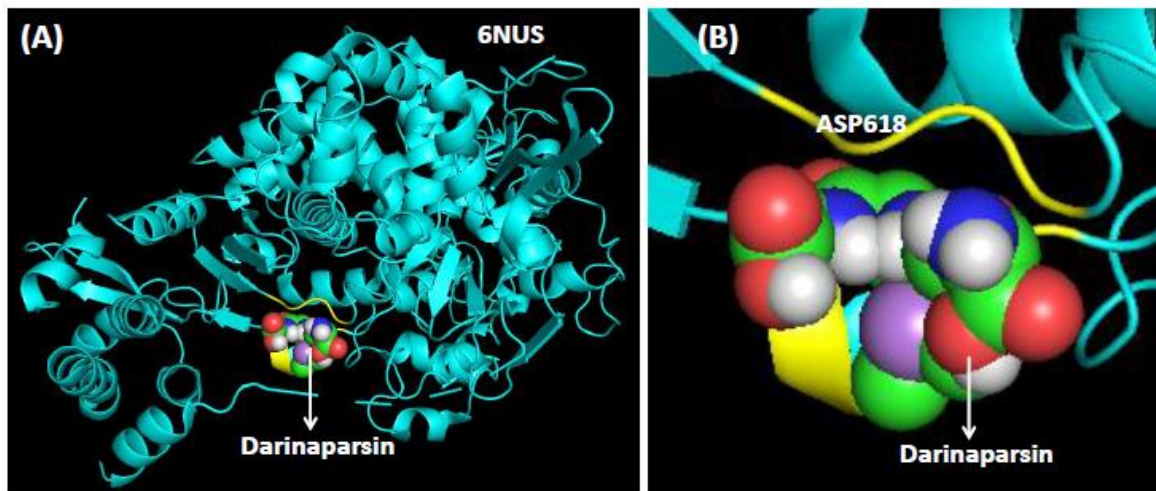
456

457

458

459

460



461

462

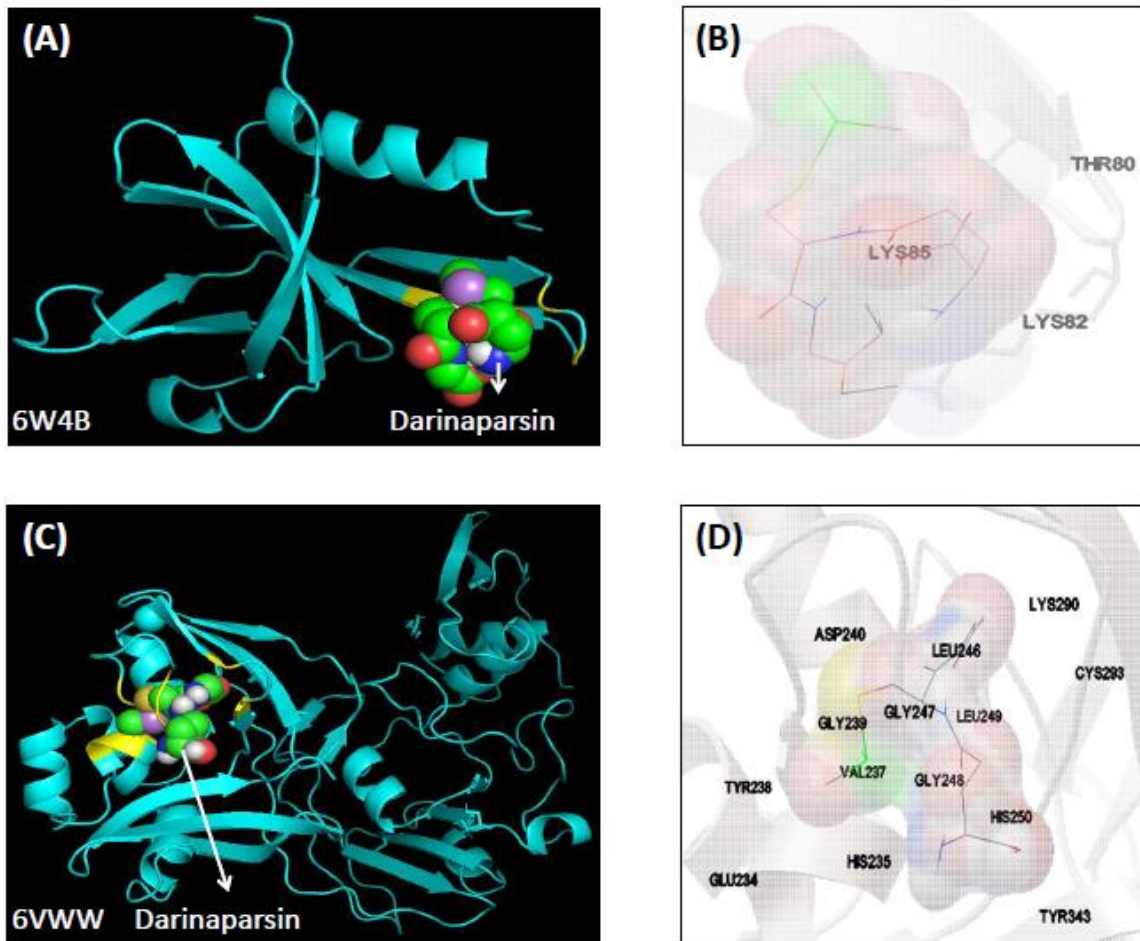
463 Figure 1

464

465

466

467



468

469 **Figure 2.**

470

471

472

473

474

475

476

477

478

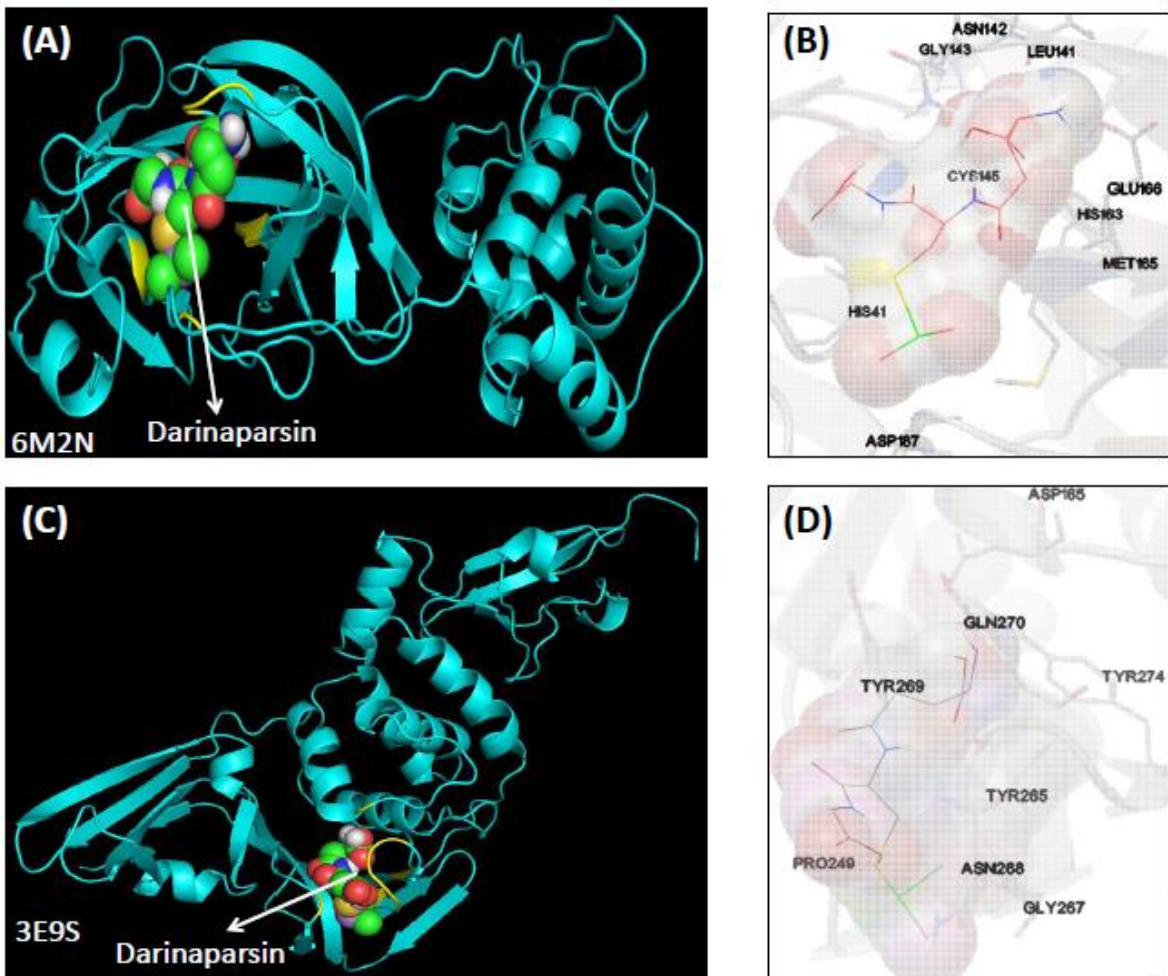
479

480

481

482

483



484

485 Figure 3.

486

487

488

489

490

491

492

493

494

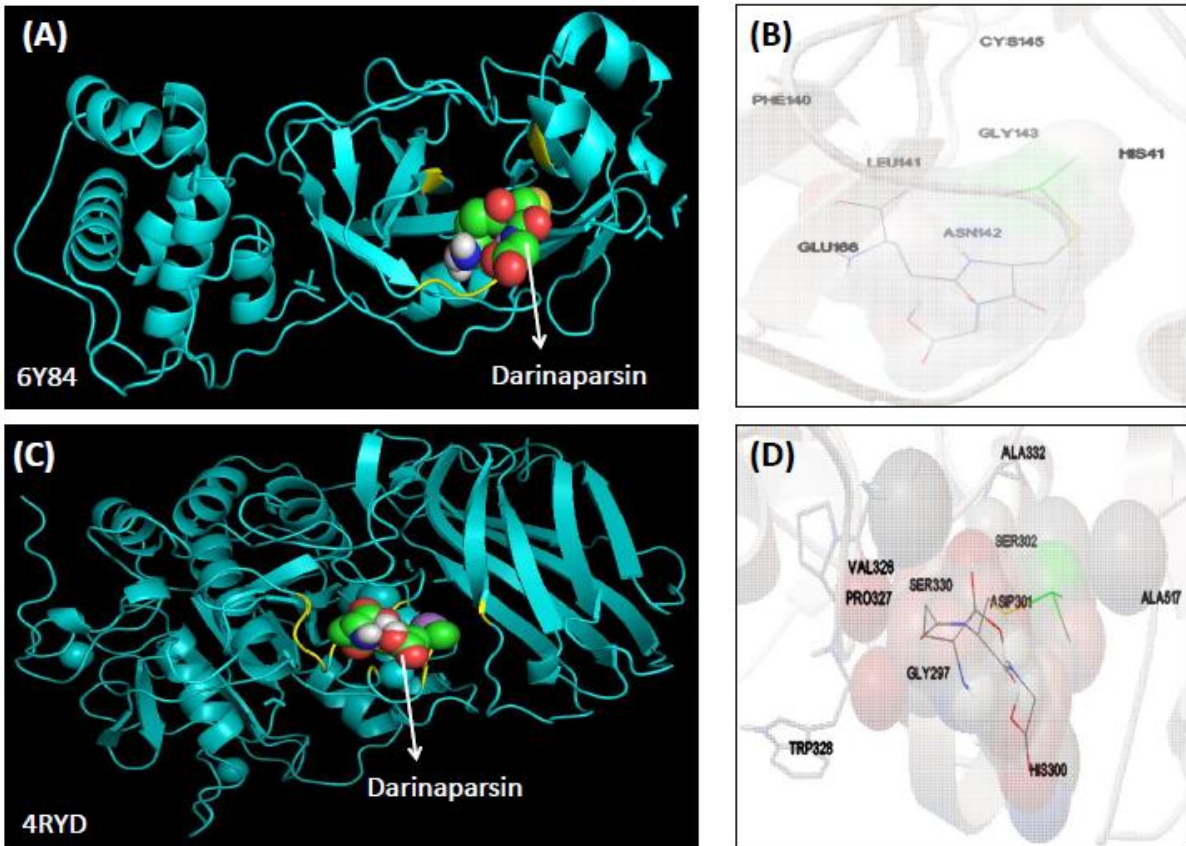
495

496

497

498

499



500

501

502 Figure 4.

503

504

505

506

507

508

509

510

511

512

513

514